 CMC, vol.4, no.3, pp.137-151, 2006

FEM-analysis of nonclassical transmission conditions between elastic structures. Part 2: Stiff imperfect interface

G. Mishuris[1], A. Öchsner[2] and G. Kuhn[3]

Abstract: Nonclassical transmission conditions for dissimilar elastic structures with imperfect interfaces are investigated. The thin interface zone is assumed to be soft or stiff in comparison with the bonded materials and the transmission conditions for stiff interfaces are evaluated based on asymptotic analysis. The accuracy of the transmission conditions is clarified not only in terms of asymptotic estimate, but, which is especially important for users, also in values by accurate FEM calculations. The ranges of applicability of the conditions are discussed.

keyword: Elasticity, Imperfect interface, Nonclassical transmission conditions, Finite element method

1 Introduction

In the first part of the paper Mishuris (2005b), symmetrical elastic structures consisting of two thick layers matched by a thin interphase layer exhibiting different material properties under conditions of simple shear and tensile loading have been considered. Transmission conditions for the soft interface have been analytically evaluated there by asymptotic analysis to compare with the results obtained by FEM analysis of the structure. It has been shown that the numerical error in these special cases is essentially smaller than it could be expected from the theory. Even in the case of the stiff interface, where other transmission conditions should rather be applied, satisfying agreement has been obtained. In this paper, dissimilar elastic structures have been analysed under different loading (simple or complex one) by the same FEM techniques. Additionally, transmission conditions for the stiff interface will be evaluated by asymptotic methods and later numerically verified in order to estimate the possible error connected with its application. Finally, such important values, for practical numerical calculations dealing with bimaterial structures with thin interfaces, as ranges of edge effect zone, validity of the discussed transmission conditions and singularity dominated zone will be evaluated. These effects are the main reason for cracking and delamination in composite materials [Akisania (1997); Boichuk (2001); Kokhanenko (2003); Li (2004); Qian (1998); Yu (2001)].

[1] RzUT, Rzeszow, POLAND.
[2] UA, Aveiro, PORTUGAL.
[3] FAU, Erlangen, GERMANY.

2 Asymptotic evaluation of transmission conditions between two elastic materials with a stiff elastic interphase (2D-problem)

Let us consider a model plane problem for a bimaterial elastic solid in the rectangle $\Omega_h = \Omega_+ \cup \Omega_- \cup \Omega$, where $\Omega_\pm = \{(x,y), \pm y \geq h\}$, $\Omega = \{(x,y), |y| \leq h\}$ (see Fig. 1). We assume that the intermediate layer Ω is inhomogeneous and isotropic, while the bonded materials are isotropic and homogeneous. Let $\mathbf{u}_\pm(x,y)$ and $\mathbf{u}(x,y)$ be vectors of displacements: $\mathbf{u}_\pm = [u_x^\pm, u_y^\pm]^\top$, $\mathbf{u} = [u_x, u_y]^\top$.

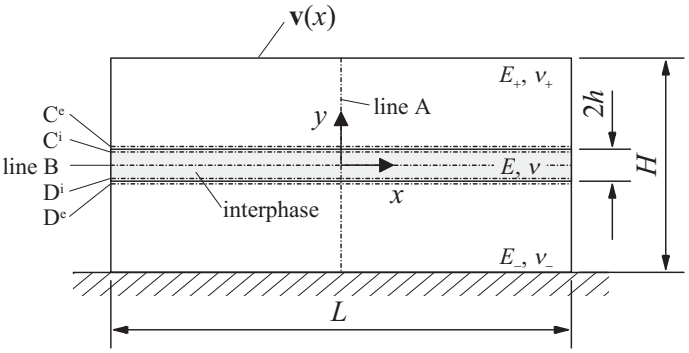

Figure 1 : Schematic representation of evaluation paths and boundary conditions of the investigated structure

They satisfy Lamé equations in the corresponding domains :

$$\mathcal{L}_\pm \mathbf{u}_\pm = \mathbf{0}, \quad (x,y) \in \Omega_\pm, \qquad \mathcal{L}\mathbf{u} = \mathbf{0}, \quad (x,y) \in \Omega, \qquad (1)$$

where the differential operators $\mathcal{L}_\pm$ and $\mathcal{L}$ are defined in

the following manner:

$$\mathcal{L}_{\pm}=\begin{pmatrix}(\lambda_{\pm}+2\mu_{\pm})D_x^2+\mu_{\pm}D_y^2 & (\lambda_{\pm}+\mu_{\pm})D_xD_y\\ (\lambda_{\pm}+\mu_{\pm})D_xD_y & (\lambda_{\pm}+2\mu_{\pm})D_y^2+\mu_{\pm}D_x^2\end{pmatrix}, \tag{2}$$

$$\mathcal{L}=\begin{pmatrix}D_x(\lambda+2\mu)D_x+D_y\mu D_y & D_x\lambda D_y+D_y\mu D_x\\ D_y\lambda D_x+D_x\mu D_y & D_y(\lambda+2\mu)D_y+D_x\mu D_x\end{pmatrix}, \tag{3}$$

where D_x and D_y denote respective partial derivatives.

On the exterior boundary some boundary conditions are assumed to be satisfied:

$$\mathcal{B}_{\pm}\mathbf{u}_{\pm}=\mathbf{0},\quad (x,y)\in\partial\Omega_h\cap\partial\Omega_{\pm},$$

$$\mathcal{B}\mathbf{u}=\mathbf{0},\quad (x,y)\in\partial\Omega_h\cap\partial\Omega. \tag{4}$$

We do not precise here the forms of the boundary operators $\mathcal{B}_{\pm}$ and $\mathcal{B}$, because they will not play any role in the formal asymptotic procedure. However, they are very important, of course, in order to prove the final asymptotic estimate for the asymptotic solution obtained in some functional spaces.

Along the interior boundaries, i.e. $y=\pm h$, the perfect transmission conditions should be satisfied:

$$\mathbf{u}_{\pm}(x,\pm h)=\mathbf{u}(x,\pm h),\quad \sigma_{\pm}^{(y)}(x,\pm h)=\sigma^{(y)}(x,\pm h), \tag{5}$$

where

$$\sigma_{\pm}^{(y)}(x,y)=\mathcal{M}_{\pm}\mathbf{u}_{\pm}(x,y),\quad \sigma^{(y)}(x,y)=\mathcal{M}\mathbf{u}(x,y), \tag{6}$$

$$\mathcal{M}_{\pm}=\begin{pmatrix}\mu_{\pm}D_y & \mu_{\pm}D_x\\ \lambda_{\pm}D_x & (\lambda_{\pm}+2\mu_{\pm})D_y\end{pmatrix},$$

$$\mathcal{M}=\begin{pmatrix}\mu D_y & \mu D_x\\ \lambda D_x & (\lambda+2\mu)D_y\end{pmatrix}. \tag{7}$$

Let us assume that the intermediate layer is essentially thinner in comparison with the characteristic size of the body: $h<<\min\{L,H\}$. This allows us to introduce in the problem a small dimensionless parameter $\varepsilon<<1$ in the following manner:

$$\varepsilon h_0=h \tag{8}$$

and rescale the variable within the intermediate layer:

$$(x,y)\in\Omega\quad y=\varepsilon\xi,\qquad \xi\in[-h_0,h_0],\quad h_0\sim\min\{L,H\}. \tag{9}$$

We assume through out this section that the interphase material is essentially stiffer in comparison with both bonded materials:

$$\mu(x,y)=\varepsilon^{-1}\mu_0(x,\xi),\ \ \lambda(x,y)=\varepsilon^{-1}\lambda_0(x,\xi),\quad \mu_0\sim\mu_{\pm}, \tag{10}$$

and denote by $\mathbf{w}(x,\xi)=\mathbf{u}(x,\varepsilon\xi)$ the solution within the domain $\Omega_0=\{(x,\xi),\ |\xi|\le h_0\}$. In this new notation, all operators can be rewritten as follows:

$$\mathcal{L}=\varepsilon^{-3}\mathcal{L}_0+\varepsilon^{-2}\mathcal{L}_1+\varepsilon^{-1}\mathcal{L}_2,\ \ \mathcal{M}=\varepsilon^{-2}\mathcal{M}_0+\varepsilon^{-1}\mathcal{M}_1, \tag{11}$$

where

$$\mathcal{L}_0=D_{\xi}\mathbf{A}_0D_{\xi}, \tag{12}$$

$$\mathcal{L}_1=\begin{pmatrix}0 & D_x\lambda_0D_{\xi}+D_{\xi}\mu_0D_x\\ D_{\xi}\lambda_0D_x+D_x\mu_0D_{\xi} & 0\end{pmatrix}, \tag{13}$$

$$\mathcal{L}_2=D_x\mathbf{A}_2D_x,\quad \mathcal{M}_0=\mathbf{A}_0D_{\xi},\quad \mathcal{M}_1=\mathbf{A}_1D_x, \tag{14}$$

$$\mathbf{A}_0=\begin{pmatrix}\mu_0 & 0\\ 0 & \lambda_0+2\mu_0\end{pmatrix},\quad \mathbf{A}_1=\begin{pmatrix}0 & \mu_0\\ \lambda_0 & 0\end{pmatrix},$$

$$\mathbf{A}_2=\begin{pmatrix}\lambda_0+2\mu_0 & 0\\ 0 & \mu_0\end{pmatrix}. \tag{15}$$

Then, a part of the problem under consideration within the domain Ω_0 can be reformulated in the following manner: we should seek for the solution $\mathbf{w}$ in the domain Ω_0 satisfying the equation:

$$\Big(\mathcal{L}_0+\varepsilon\mathcal{L}_1+\varepsilon^2\mathcal{L}_2\Big)\mathbf{w}=\mathbf{0},\quad (x,\xi)\in\Omega_0, \tag{16}$$

and the interior transmission conditions:

$$\mathbf{u}_{\pm}(x,\pm\varepsilon h_0)=\mathbf{w}(x,\pm h_0),$$

$$\varepsilon^2\sigma_{\pm}^{(y)}(x,\pm\varepsilon h_0)=\Big(\mathcal{M}_0+\varepsilon\mathcal{M}_1\Big)\mathbf{w}|_{\xi=\pm h_0}. \tag{17}$$

The solution within the corresponding domains will be sought in form of asymptotic series:

$$\mathbf{w}(x,\xi)=\sum_{j=0}^{\infty}\varepsilon^j\mathbf{w}_j(x,\xi),\quad \mathbf{u}_{\pm}(x,y)=\sum_{j=0}^{\infty}\varepsilon^j\mathbf{u}_j^{\pm}(x,y). \tag{18}$$

As a result, sequence of the BVPs determining respective terms in the asymptotic expansions (18) will be found. Thus, for the first term $\mathbf{w}_0$ one can obtain:

$$D_\xi\mathbf{A}_0D_\xi\mathbf{w}_0=\mathbf{0},\quad (x,\xi)\in\Omega_0, \tag{19}$$

$$\mathbf{u}_0^{\pm}(x,\pm 0)=\mathbf{w}_0(x,\pm h_0), \tag{20}$$

$$\mathbf{A}_0D_\xi\mathbf{w}_0|_{\xi=\pm h_0}=\mathbf{0}. \tag{21}$$

From (19) and (21) one can obtain that

$$\mathbf{w}_0(x,\xi)=\mathbf{a}_1(x), \tag{22}$$

while the unknown function $\mathbf{a}_1(x)$ has to be found from (20):

$$\mathbf{a}_1(x)=\mathbf{u}_0^-(x,-0), \tag{23}$$

and an additional condition has to be satisfied:

$$[\mathbf{u}_0]_{y=0}\equiv\mathbf{u}_0^+(x,+0)-\mathbf{u}_0^-(x,-0)=\mathbf{0}. \tag{24}$$

Note that equation (24) constitutes the first unknown imperfect transmission condition for the external solutions $\mathbf{u}_0^{\pm}$ within the bonded materials.

To find the next sought for the transmission condition for the first term of the external asymptotic expansion, $\mathbf{u}_0^{\pm}$, one can continue the procedure to analyse the second internal BVP:

$$D_\xi\mathbf{A}_0D_\xi\mathbf{w}_1+\mathcal{L}_1\mathbf{w}_0=\mathbf{0},\quad (x,\xi)\in\Omega_0, \tag{25}$$

$$\pm h_0D_y\mathbf{u}_0^{\pm}(x,\pm 0)+\mathbf{u}_1^{\pm}(x,\pm 0)=\mathbf{w}_1(x,\pm h_0), \tag{26}$$

$$\mathbf{A}_0D_\xi\mathbf{w}_1|_{\xi=\pm h_0}+\mathcal{M}_1\mathbf{w}_0|_{\xi=\pm h_0}=\mathbf{0}. \tag{27}$$

Taking into account the properties (22) of the internal solution $\mathbf{w}_0$, one can rewrite equations (25) and (27) in equivalent forms:

$$D_\xi\mathbf{A}_0D_\xi\mathbf{w}_1+D_\xi\mathbf{A}_1D_x\mathbf{w}_0=\mathbf{0},\quad (x,\xi)\in\Omega_0, \tag{28}$$

$$\mathbf{A}_0D_\xi\mathbf{w}_1|_{\xi=\pm h_0}+\mathbf{A}_1D_x\mathbf{w}_0|_{\xi=\pm h_0}=\mathbf{0}. \tag{29}$$

The solution to this problem is easily calculated as:

$$\mathbf{w}_1(x,\xi)=\mathbf{a}_2(x)-\int_0^{\xi}\mathbf{A}_0^{-1}(x,t)\mathbf{A}_1(x,t)dt\cdot D_x\mathbf{w}_0(x), \tag{30}$$

where

$$\mathbf{a}_2(x)=\int_0^{-h_0}\mathbf{A}_0^{-1}(x,t)\mathbf{A}_1(x,t)dt\cdot D_x\mathbf{w}_0(x) -h_0D_y\mathbf{u}_0^-(x,-0)+\mathbf{u}_1^-(x,-0), \tag{31}$$

and an additional transmission condition has to be satisfied for the solution $\mathbf{u}_1$ of the second external BVP:

$$[\mathbf{u}_1]_{y=0}=-\int_{-h_0}^{h_0}\mathbf{A}_0^{-1}(x,t)\mathbf{A}_1(x,t)dt\cdot D_x\mathbf{w}_0(x) -2h_0\langle D_y\mathbf{u}_0\rangle_{y=0}. \tag{32}$$

There, we have introduced the standard notation

$$\langle f\rangle=\frac{1}{2}(f_++f_-). \tag{33}$$

As it follows from this step, it is not enough to consider even the second term of the internal asymptotic expansion, $\mathbf{w}_1$, to find the still missing transmission solution for the first term of the external expansion, $\mathbf{u}_0^{\pm}$. Thus, one needs to continue the asymptotic procedure. Let us consider the internal BVP for the third term of the internal asymptotic expansion (18):

$$D_\xi\mathbf{A}_0D_\xi\mathbf{w}_2+\mathcal{L}_1\mathbf{w}_1+\mathcal{L}_2\mathbf{w}_0=\mathbf{0},\quad (x,\xi)\in\Omega_0, \tag{34}$$

$$\frac{1}{2}h_0^2D_y^2\mathbf{u}_0^{\pm}(x,\pm 0)\pm h_0D_y\mathbf{u}_1^{\pm}(x,\pm 0)+\mathbf{u}_2^{\pm}(x,\pm 0) =\mathbf{w}_2(x,\pm h_0), \tag{35}$$

$$\boldsymbol{\sigma}_0^{(y\pm)}(x,0)=\mathbf{A}_0D_\xi\mathbf{w}_2|_{\xi=\pm h_0}+\mathcal{M}_1\mathbf{w}_1|_{\xi=\pm h_0}. \tag{36}$$

Equations (34) and (36) can be simplified using the results from the previous steps:

$$D_\xi\mathbf{A}_0D_\xi\mathbf{w}_2+D_\xi\mathbf{A}_1D_x\mathbf{w}_1+D_x\mathbf{A}_3D_x\mathbf{w}_0=\mathbf{0},\quad (x,\xi)\in\Omega_0, \tag{37}$$

$$\boldsymbol{\sigma}_0^{(y\pm)}(x,0)=\mathbf{A}_0D_\xi\mathbf{w}_2|_{\xi=\pm h_0}+\mathbf{A}_1D_x\mathbf{w}_1|_{\xi=\pm h_0}, \tag{38}$$

where we have introduced a new notation:

$$\mathbf{A}_3=\tau\begin{pmatrix}1&0\\0&0\end{pmatrix},\quad \tau=\frac{4\mu_0(\lambda_0+\mu_0)}{\lambda_0+2\mu_0}=\frac{2\mu_0}{1-\nu_0}. \tag{39}$$

Equation (38) can be integrated to give:

$$\mathbf{A}_0 D_\xi \mathbf{w}_2 + \mathbf{A}_1 D_x \mathbf{w}_1 = \mathbf{a}_3(x) - D_x \int_0^\xi \mathbf{A}_3(x,t)dt \cdot D_x \mathbf{w}_0, \quad (x,\xi) \in \Omega_0. \quad (40)$$

From this equation and (38) one can immediately conclude that

$$[\sigma_0^{(y)}]_{y=0} + D_x \int_{-h_0}^{h_0} \mathbf{A}_3(x,t)dt \cdot D_x \mathbf{w}_0 = \mathbf{0}. \quad (41)$$

However, taking into account relations (22)-(24), last equation can be rewritten in the form:

$$[\sigma_0^{(y)}]_{y=0} + D_x \int_{-h_0}^{h_0} \mathbf{A}_3(x,t)dt \cdot D_x \mathbf{u}_0|_{y=0} = \mathbf{0}, \quad (42)$$

which constitutes together with (24) the sought for necessary transmission conditions for the first external BVP in the case of the stiff interface.

Summarizing the obtained result with those concerning imperfect transmission conditions from [Antipov (2001); Movchan (1995); Mishuris (2005b)] one can collect them together within Table 1. It is assumed that the imperfect interface is always situated along the coordinate line $y = 0$.

Table 1 : Possible sets of transmission conditions depending on the relative properties of the thin intermediate layer: 2-D problems

interface		
soft	comparable	stiff
$[u_x] - a_2\sigma_{xy} = 0$	$[u_x] = 0$	$[u_x] = 0$
$[u_y] - a_1\sigma_y = 0$	$[u_y] = 0$	$[u_y] = 0$
$[\sigma_{xy}] = 0$	$[\sigma_{xy}] = 0$	$[\sigma_{xy}] + \frac{\partial}{\partial x}\left(a_3 \frac{\partial u_x}{\partial x}\right) = 0$
$[\sigma_y] = 0$	$[\sigma_y] = 0$	$[\sigma_y] = 0$

Here, the parameters a_j in formulae from Table 1 are, generally speaking, functions with respect to the variable x and have to be calculated according to the equations in Table 2. Under the additional assumption that the material properties of the interface do not vary in direction perpendicular to the interface (do not depend on variable y in this case) these equations can be simplified and rewritten in forms presented in Table 3, where all mechanical and geometrical parameters can be only functions of variable x (change its values only along the imperfect interface).

Table 2 : General representation of the parameters $a_j(x)$ in Table 1 for plane strain and plane stress case

case	plane strain	plane stress
$a_1(x)$	$\int_{-h}^{h} \frac{(1+\nu)(1-2\nu)}{E(1-\nu)} dy$	$\int_{-h}^{h} \frac{(1-\nu^2)}{E} dy$
$a_2(x)$	$\int_{-h}^{h} \frac{2(1+\nu)}{E} dy$	$\int_{-h}^{h} \frac{2(1+\nu)}{E} dy$
$a_3(x)$	$\int_{-h}^{h} \frac{E}{1-\nu^2} dy$	$\int_{-h}^{h} E\, dy$

Table 3 : Particular representation of the parameters $a_j(x)$ in Table 1 for plane strain and plane stress case

case	plane strain	plane stress
$a_1(x)$	$\frac{2h(1+\nu)(1-2\nu)}{E(1-\nu)}$	$\frac{2h(1-\nu^2)}{E}$
$a_2(x)$	$\frac{4h(1+\nu)}{E}$	$\frac{4h(1+\nu)}{E}$
$a_3(x)$	$\frac{2hE}{1-\nu^2}$	$2hE$

3 Numerical results

3.1 *Dissimilar layer with soft imperfect interface under simple shear and tensile loading*

Let us consider a dissimilar elastic structure with a thin elastic interphase which exhibits other properties than the bonded materials (Fig. 1). The thickness of the interface zone is assumed to be small $\varepsilon = 2h/H = 0.01$ and this value will be considered through out the paper as a small parameter. In this subsection, results similar to those presented in paper [Mishuris (2005b)] will be evaluated. The only difference is now that the matched materials are not the same. The top part of the structure is represented by steel with elastic constants $E_+ = 210000$ MPa, $\nu_+ = 0.3$, while the bottom part is of aluminum ($E_- = 72700$

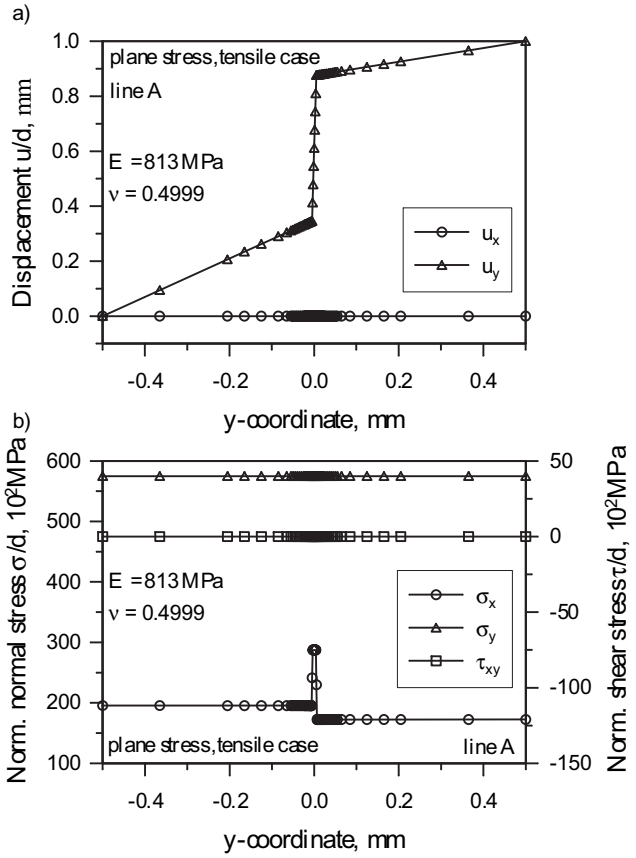

Figure 2 : Displacement and stress distribution along line A for the asymmetric sample and the simple tensile loading

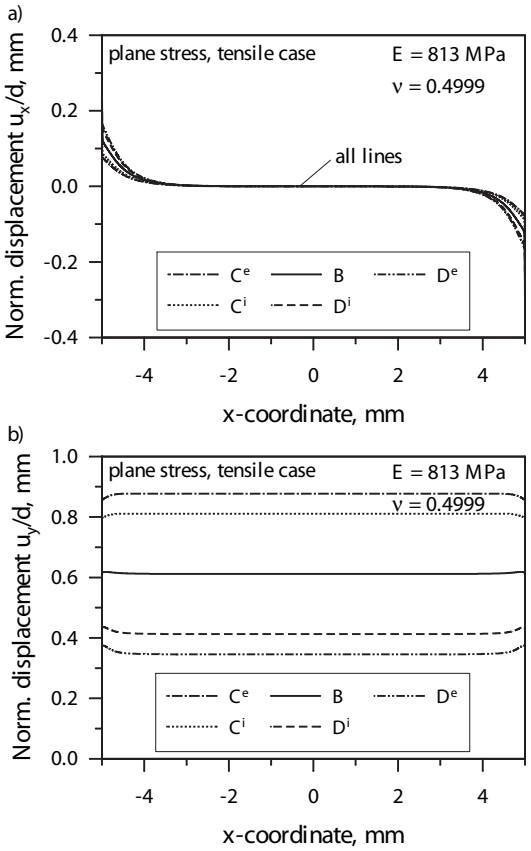

Figure 3 : Displacement distribution along lines B, C and D for the asymmetric sample and the simple tensile loading

MPa, $\nu_{-} = 0.34$). Various elastic constants for the interphase material are considered in the same way as it has been done in Mishuris (2005b) for easy comparison of the obtained results. First, simple tensile and simple shear loadings are considered: $v_x(x) = 0$, $v_y(x) = 1 \cdot d$ (where d is an arbitrary dimensionless parameter for normalization) and $v_x(x) = 1 \cdot d$, $v_y(x) = 0$, respectively. All calculations have been done by the FE code MSC.Marc. For details concerning the constructed FEM-mesh for the considered structure we refer the reader to the first part of the paper [Mishuris (2005b)].

In Figs. 2, 3 and 4, the normalized distributions of the displacements and the stresses in direction perpendicular to the interface (along the line A) and along the interface (lines B, C^e, C^i, D^e, D^i) are presented (see Fig. 1 for the used notations). The material parameters of the soft weakly compressible intermediate layer in this case are: $E = 813$ MPa, $\nu = 0.4999$ (the same as in paper

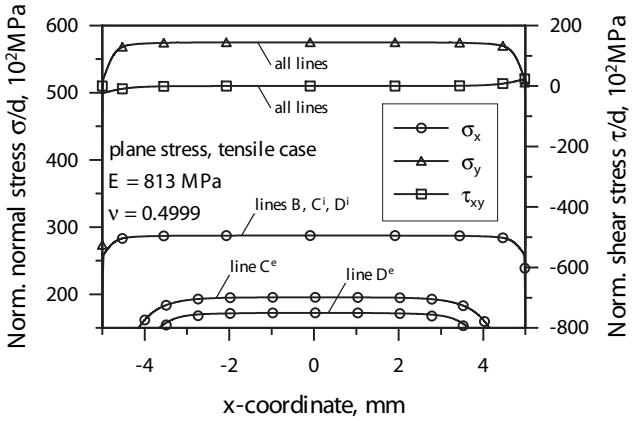

Figure 4 : Normal and shear stress distribution along horizontal lines B, C and D for the asymmetric sample and the simple tensile loading

[Mishuris (2005b)] for the reason of comparison).

It is easy to see that the solution has lost its symme-

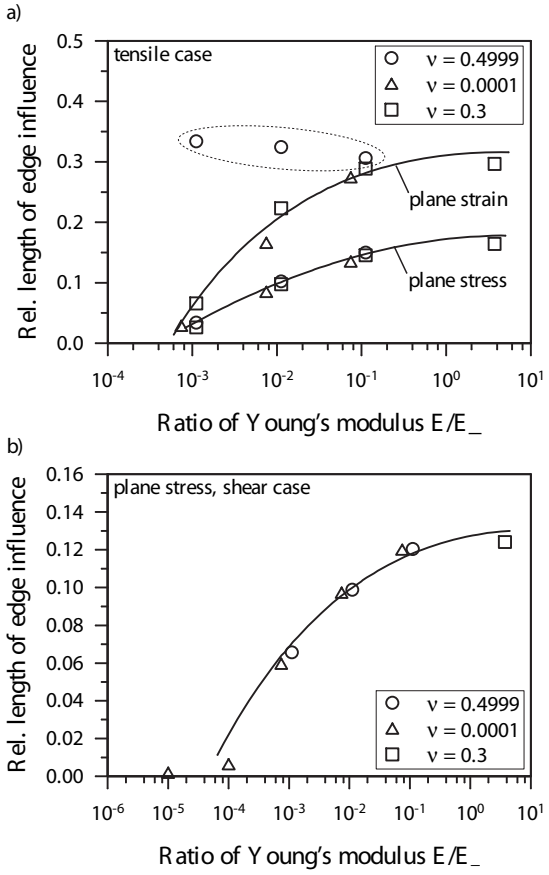

Figure 5 : Relative length of the edge effect zone for the asymmetric sample

try which is natural to the problem definition. However, because of simple tensile loading, displacements and stresses on lines B, C^e, C^i, D^e, D^i are still practically constants along the major part of the imperfect interface. This enables us to easily define the size of the edge zone with the same 1% accuracy criterion from changing the constant behavior of the traction along the interface. Corresponding results are included in Fig. 5. Similarly as in the symmetrical case, only the weakly compressible interface for the plane strain case under tensile loading exhibits irregular behavior in comparison with all other cases.

Let us note that there is no practical difference in the case of the shear loading for plane strain and plane stress states. This phenomenon has been explained in [Mishuris (2005b)], and is a simple consequence of the fact that the components of both solutions responsible for the shear deformation satisfy the same equations, boundary and transmission conditions (cf. Table 1). Because of this fact, we present here in Fig. 5b only the plane stress case. On the other hand, the straight line behavior of the solution within the sample give us an occasion to restrict our interest to the accuracy of the transmission conditions in one point and we have chosen the symmetry point $x = 0$ in the middle of the rectangle, i.e. the same point as in [Mishuris (2005b)]. Corresponding results have been collected in Tables 4-7. In Table 7 for the plane strain case we have presented one case for comparison with Table 6.

Within the edge zone, the behavior of the solutions for the dissimilar body may essentially differ in comparison with the symmetrical case due to the distinct limited asymptotic behavior of the solution near the corner points of the intermediate layer and the external boundary (intersection points). This fact is manifested by Fig. 3. However, even within the edge effect zone, the corresponding transmission transmission conditions from Table 1 are still valid. We discuss this phenomenon in details later in the fourth subsection.

3.2 Dissimilar layer with soft imperfect interface under complex loading.

In the first part of this paper [Mishuris (2005b)], only symmetrical structures with simple external loading, i.e. simple tensile or simple shear, were considered for a soft interphase and the accuracy of the transmission conditions turned out to be much better than one could expect from the theoretical point of view. In order to investigate if this fact was based on the simple cases under consideration, we are going to investigate in this subsection the influence of complex loading on the accuracy of the transmission conditions for asymmetric samples. First of all, it is necessary to underline once again that the conditions checked up till now numerically, have been satisfied with an error smaller than that predicted from the asymptotic theory. We are going to show now that this is because of the applied simple loading and, in case of a complex one, the theoretical predictions simply coincide with the numerical calculations.

Let us consider a more complicated tensile loading in the same dissimilar structure with the same soft interface as in the previous subsection. Namely, instead of the uniform external loading, a complex tensile loading defined as follows: $u_y(x,h/2) = v_y(x) = dx^2/25$, $v_x(x) = 0$ is applied in the plane stress case.

Numerical results in graphical form for such loading,

Table 4 : Relative errors for the second and fourth transmission conditions from Table 1 for the asymmetric plane stress simple tensile case along line A

E	ν	$\frac{\Delta u_y(0,0)}{\sigma_y(0,0)}$	$\frac{2h(1-\nu^2)}{E}$	rel. error	$\frac{\Delta\sigma_y(0,0)}{\sigma_y(0,0)}$
8138	0.4999	$9.217259\cdot10^{-7}$	$9.217252\cdot10^{-7}$	$6.916\cdot10^{-7}$	$-9.088\cdot10^{-9}$
813	0.4999	$9.226338\cdot10^{-6}$	$9.226322\cdot10^{-6}$	$1.735\cdot10^{-6}$	$-3.479\cdot10^{-8}$
81	0.4999	$9.260510\cdot10^{-5}$	$9.260494\cdot10^{-5}$	$1.724\cdot10^{-7}$	$-1.008\cdot10^{-8}$
5427	0.0001	$1.842648\cdot10^{-6}$	$1.842639\cdot10^{-6}$	$5.084\cdot10^{-6}$	$-1.001\cdot10^{-8}$
542	0.0001	$1.845021\cdot10^{-5}$	$1.845018\cdot10^{-5}$	$1.538\cdot10^{-6}$	$-2.662\cdot10^{-8}$
54	0.0001	$1.851854\cdot10^{-4}$	$1.851852\cdot10^{-4}$	$1.286\cdot10^{-6}$	$-1.934\cdot10^{-8}$
8138	0.3000	$1.118216\cdot10^{-6}$	$1.118211\cdot10^{-6}$	$4.183\cdot10^{-6}$	$-9.285\cdot10^{-9}$
813	0.3000	$1.119313\cdot10^{-5}$	$1.119311\cdot10^{-5}$	$1.404\cdot10^{-6}$	$-1.936\cdot10^{-8}$
81	0.3000	$1.123458\cdot10^{-4}$	$1.123457\cdot10^{-4}$	$1.450\cdot10^{-7}$	$-1.205\cdot10^{-8}$
271270	0.3000	$3.354742\cdot10^{-8}$	$3.354591\cdot10^{-8}$	$4.490\cdot10^{-4}$	$-2.460\cdot10^{-8}$

Table 5 : Relative errors for the second and fourth transmission conditions from Table 1 for the asymmetric plane strain simple tensile case along line A

E	ν	$\frac{\Delta u_y(0,0)}{\sigma_y(0,0)}$	$\frac{2h(1+\nu)(1-2\nu)}{E(1-\nu)}$	rel. error	$\frac{\Delta\sigma_y(0,0)}{\sigma_y(0,0)}$
8138	0.4999	$7.472625\cdot10^{-10}$	$7.370853\cdot10^{-10}$	$1.362\cdot10^{-2}$	$2.465\cdot10^{-5}$
813	0.4999	$7.387995\cdot10^{-9}$	$7.378106\cdot10^{-9}$	$1.195\cdot10^{-3}$	$3.102\cdot10^{-5}$
81	0.4999	$7.407831\cdot10^{-8}$	$7.405432\cdot10^{-8}$	$3.238\cdot10^{-4}$	$1.119\cdot10^{-5}$
5427	0.0001	$1.842650\cdot10^{-6}$	$1.842639\cdot10^{-6}$	$5.980\cdot10^{-6}$	$-1.122\cdot10^{-7}$
8138	0.3000	$9.128290\cdot10^{-7}$	$9.128252\cdot10^{-7}$	$4.142\cdot10^{-6}$	$-1.205\cdot10^{-7}$

Table 6 : Relative errors for the second and fourth transmission conditions from Table 1 for the asymmetric plane stress simple shear case along line A

E	ν	$\frac{\Delta u_x(0,0)}{\sigma_{xy}(0,0)}$	$\frac{4h(1+\nu)}{E}$	rel. error	$\frac{\Delta\sigma_{xy}(0,0)}{\sigma_{xy}(0,0)}$
8138	0.4999	$3.686151\cdot10^{-6}$	$3.686164\cdot10^{-6}$	$-3.381\cdot10^{-6}$	$5.612\cdot10^{-8}$
813	0.4999	$3.689783\cdot10^{-5}$	$3.689791\cdot10^{-5}$	$-2.034\cdot10^{-6}$	$6.127\cdot10^{-8}$
81	0.4999	$3.703429\cdot10^{-4}$	$3.703431\cdot10^{-4}$	$-7.541\cdot10^{-6}$	$3.947\cdot10^{-8}$
5427	0.0001	$3.685663\cdot10^{-6}$	$3.685646\cdot10^{-6}$	$4.565\cdot10^{-6}$	$2.806\cdot10^{-8}$
542	0.0001	$3.690406\cdot10^{-5}$	$3.690406\cdot10^{-5}$	$-8.265\cdot10^{-8}$	$6.128\cdot10^{-8}$
54	0.0001	$3.704048\cdot10^{-4}$	$3.704074\cdot10^{-4}$	$-7.147\cdot10^{-6}$	$3.948\cdot10^{-8}$
271270	0.3000	$9.585672\cdot10^{-8}$	$9.584547\cdot10^{-8}$	$1.174\cdot10^{-4}$	$7.586\cdot10^{-7}$

Table 7 : Relative errors for the second and fourth transmission conditions from Table 1 for the asymmetric plane strain simple shear case along line A

E	ν	$\frac{\Delta u_x(0,0)}{\sigma_{xy}(0,0)}$	$\frac{4h(1+\nu)}{E}$	rel. error	$\frac{\Delta\sigma_{xy}(0,0)}{\sigma_{xy}(0,0)}$
8138	0.4999	$3.686143\cdot10^{-6}$	$3.686164\cdot10^{-6}$	$-5.665\cdot10^{-6}$	$2.806\cdot10^{-8}$

analogous to those in Figs. 2-4, are presented in Figs. 6-8. As earlier, it is easy to see that the displacements are still linearly distributed within the considered soft weakly compressible interface, while the stresses are constant in the direction perpendicular to the interface. Moreover, the stress components σ_{xy} and σ_y are continuous across the interface as it follows from Fig. 8 a) and the remaining component σ_x exhibits a discontinuous behavior, as

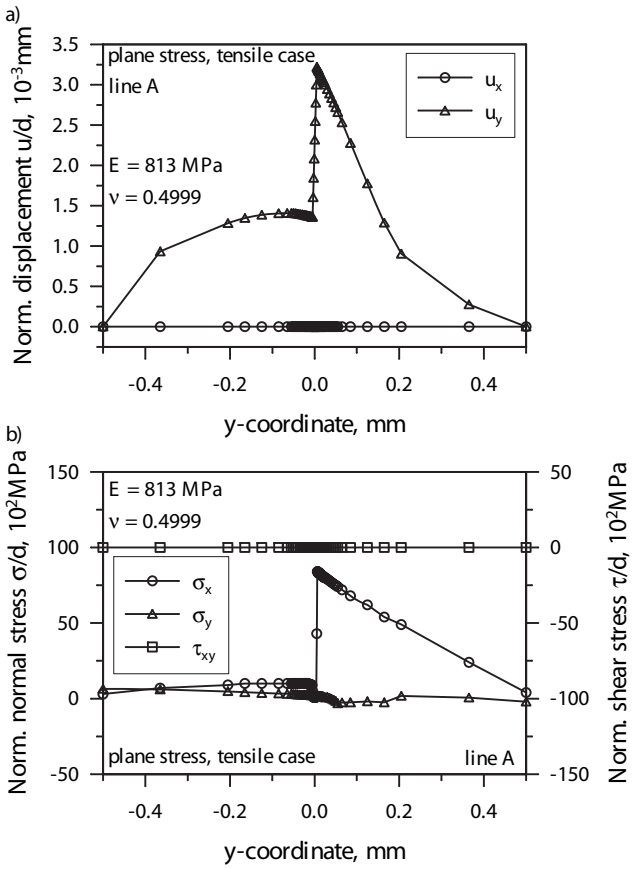

Figure 6 : Displacement and stress distribution for the asymmetric sample and the asymmetric tensile loading

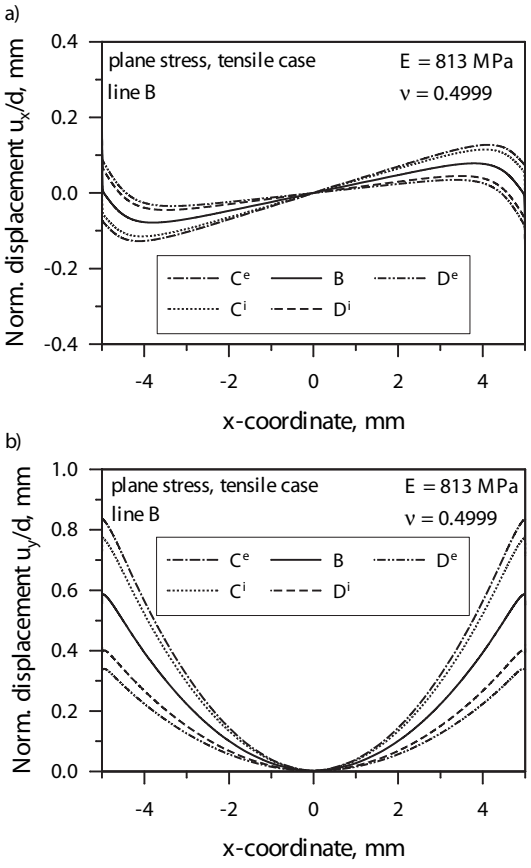

Figure 7 : Displacement distribution for the asymmetric sample and the asymmetric tensile loading along lines B, C and D

it should be expected.

However, distributions of displacement and stress components along the interface (cf. Figs. 7-8) are no longer practically constants and essentially change its behavior along the interface. Nevertheless, the vector of stresses is continuous through the interface as it follows from Fig. 8b and as it has to be according to the transmission conditions (Table 1). As a result, it is more difficult in this case to determine the edge effect zone. In the previous subsection a simple exact analytical solution has existed far away from the external edge boundary (constant stresses within each material). Now, to find the size of the edge effect zone we propose to apply another technique. Namely, we additionally load the right (and left) hand sides of the rectangle (Fig. 1) by some additional loading having zero main vectors and observe the changes in the respective solution. As we have expected, the obtained results are similar to those reported in Fig. 5 and corresponding results are presented in the first row of Table 9. One can see that the edge effect zone (calculated by the perturbation method) differs depending on which displacement or stress components it has been extracted from. However, this is not an unexpected phenomenon. For example, for the symmetrical sample and symmetrical loading, one pair of the stress and displacement components gives the edge effect zone of zero length at all due to the symmetry (cf. [Mishuris (2005b)]). In [Boichuk (2001); Kokhanenko (2003)] even the edge effect zones are determined for each component of stresses. Moreover, the sizes of the zones essentially depend on the chosen criterium. It is evident that only a crude estimation of the edge zone can be obtained in the early proposed way. Because of this, we restrict ourself in these numerical simulations to the accuracy of 0.1 in the absolute value. In the author's opinion, such information is absolutely enough to clarify the range of the phenomenon. A more important value

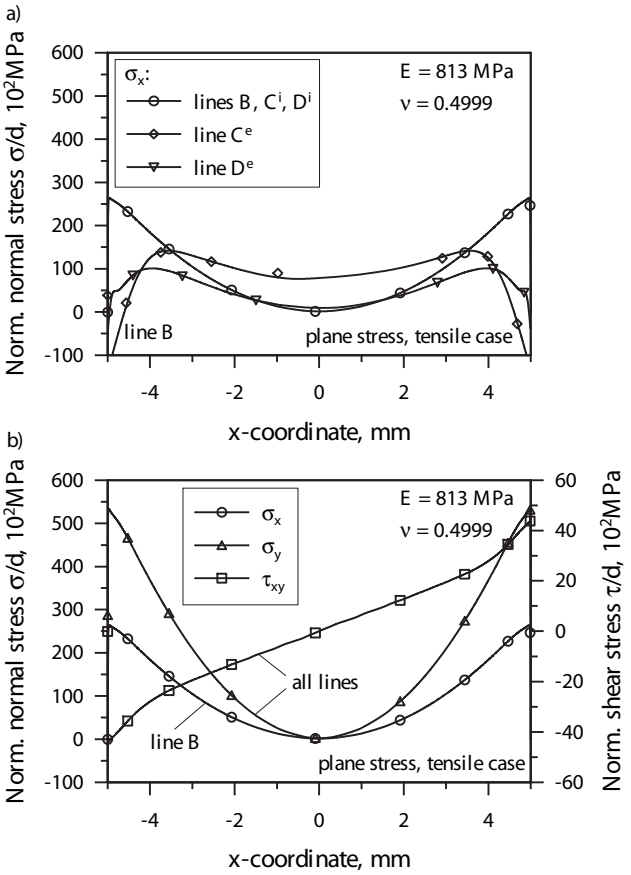

Figure 8 : Normal and shear stress distribution for the asymmetric sample and the asymmetric tensile loading along horizontal lines B, C and D

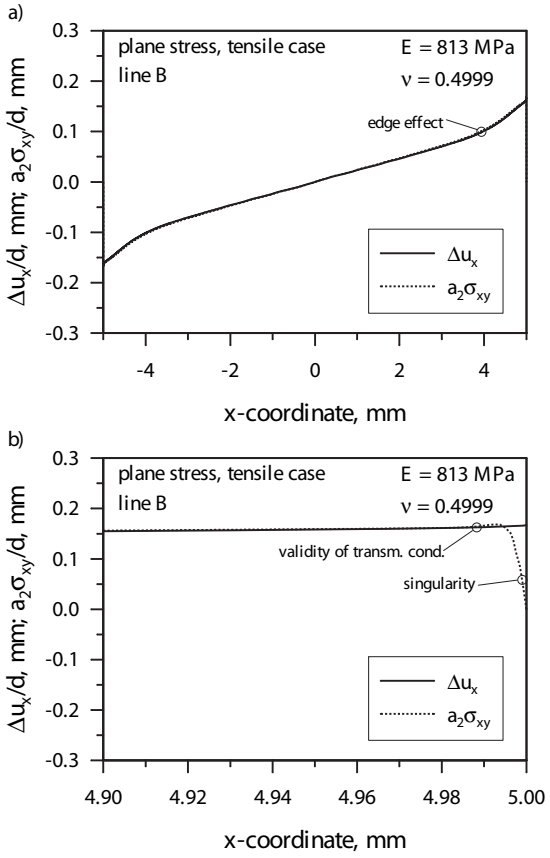

Figure 9 : Verification of the first transmission condition for the soft interface from Table 1 $(d = 1)$

for users is the size of the region where the transmission conditions hold true.

In order to find this region with a good accuracy we have additionally calculated the jumps of the corresponding displacement components from different sides of the thin interface, $[u_x]$ and $[u_y]$, and the stress components σ_{xy} and σ_y, along the middle line of the interface which have been normalized by the respective constants a_1 and a_2 according to Table 1. Corresponding results are presented in Figs. 9, 10.

One can observe a good correlation between the functions and, from the first glance, the same excellent agreement with respect to the transmission condition accuracy. However, if one wants to calculate the relative error between the values, the error has a different range in different points. This is because of the variation of the function values along the interface that makes it impossible to provide any conclusions uniquely based on the relative error estimation at any a priori chosen point, as it has been done earlier. Moreover, in the center of the sample all values even disappear with machine zero accuracy. As a result, it is impossible to directly extract the error at point $x = 0$ at all. To clarify this fact, we present in Table 8 relative errors connected with the second and the fourth transmission conditions from Table 1. The errors have been calculated in two different points at $x = 0$ (by extrapolation from the nearest points) and far away from the center (at point $x = 3.0$). From the first glance, it follows from Table 8 that the accuracy of the transmission conditions drastically changes in comparison with the previous simple loading. However, this is not an accurate conclusion.

Let us remind ourselves that the analytical estimation which has been proved for the case under consideration (the soft interface) in [Mishuris (2005b)] gives us the theoretical prediction of the order $O(\varepsilon)$. From the asymptotic analysis point of view, this only means that any

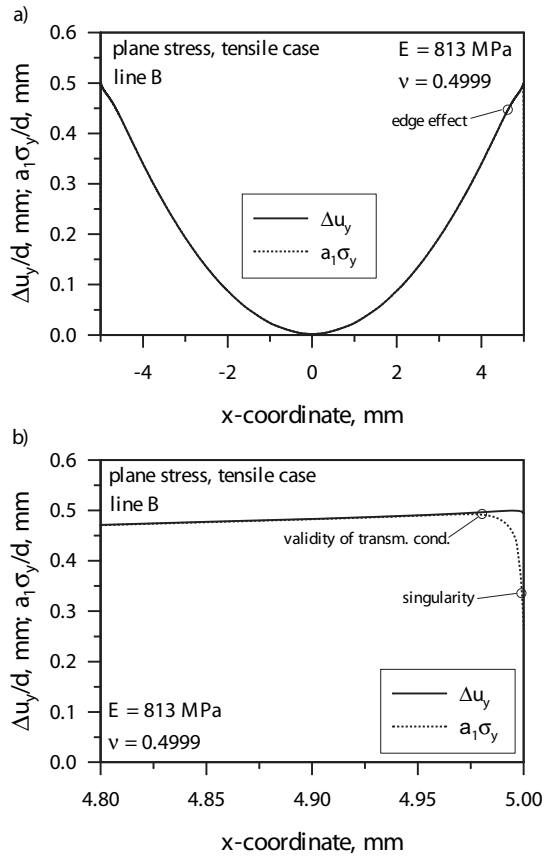

Figure 10 : Verification of the second transmission condition for the soft interface from Table 1 $(d = 1)$

value along the interface (e.g. components of the displacement or stress) is represented in the form: $z(x) = z_0(x) + \varepsilon z_1(x)$, where εz_1, in fact, is the mentioned error. However, this fact is not influenced by the relative error which is $\varepsilon z_1(x)/z(x) = O(\varepsilon)$ at an arbitrary point of the interface. This is not true, for example, near the point where $z_0(x) = 0$ holds. An appropriate approach consists in comparison of any norms of the functions that gives correct result: $||\varepsilon z_1||/||z|| = O(\varepsilon)$. Of course, in the case of a constant value ($z(x) = \text{const}$) point by point and norm definitions of the relative error coincides themselves.

Let us return to the evaluation of such value which is of extremely interest for users and researchers as the range of the validity of the nonclassical transmission conditions. Fortunately, it is still possible to determine the zone of validity of the transmission conditions with the 1% accuracy criterion based on a point by point relative error estimate starting from a point far away from the center. It is important to note that the transmission conditions are still valid within the edge effect zone. For the case under consideration the limits of the edge effect zone are marked by points in Figs. 9a and 10a. However, it is impossible to see in these figures where the transmission conditions are not valid. For this reason, we have prepared corresponding magnifications near the right-hand side of the dissimilar sample. One can easily see from the figures that the transmission conditions are still valid within the edge effect zone. The corresponding regions have been calculated with the 1% criterion and are presented in the second row of Table 10.

Let us note that there are two singular points (intersection of the interface boundaries with the external boundaries of the sample). Moreover, in the case of the dissimilar body, corresponding stress singularities are different. From the results presented in Figs. 9b and 10b one can conclude that the singularity dominated region is extremely small. Its length consists of 10^{-4} or $0.01 \cdot 2h$ that coincides with results of Akisanya reported in [Akisania (1997)]. In Figs. 9b and 10b it is easy to see that the singularity dominated region is even essentially smaller than the region where the transmission conditions are not valid. In fact, the region between the depicted points in Figs. 9b and 10b is a transmission zone between two absolutely different solution behaviors. Moreover, the singularity only appears in the respective stress term (displacement discontinuities are bonded functions). The accurate range of this zone can be calculated within the same 1% accuracy in determination of stress singularity exponent (cf. Table 9). It must be remembered that the constructed FEM mesh is very dense near the singular points.

Finally, in Table 10 norm estimate for the first two transmission conditions from Table 1 have been presented not only along the whole interface (interval (-5,5)) but also within the interval of the transmission condition validity. One can see from these results that in such a way defined relative norm error is always within range of $\varepsilon = 10^{-2}$ for the complex loading, which coincides with the theoretically predicted from the asymptotic analysis, and essentially better for the simple loading, as it has been mentioned above. Moreover, within the zone of the condition validity, the calculated integral error is an order smaller than the predicted one. Also the mentioned great influence of the applied loading on the final estimate is clearly observed.

Table 8 : Point by point verification of the transmission conditions. Plane stress, asymmetric sample and the asymmetric tensile loading, $E = 813$ MPa, $\nu = 0.4999$

x	$\frac{\Delta u_y}{\sigma_y}$	$\frac{2h(1-\nu^2)}{E}$	rel. error	$\frac{\Delta \sigma_y}{\sigma_y}$
0.0	$8.621439 \cdot 10^{-6}$	$9.226322 \cdot 10^{-6}$	$-7.016 \cdot 10^{-2}$	$-3.088 \cdot 10^{-2}$
3.0	$9.221909 \cdot 10^{-6}$	$9.226322 \cdot 10^{-6}$	$-4.785 \cdot 10^{-4}$	$-2.728 \cdot 10^{-4}$

Table 9 : Ranges of the different edge phenomena. Plane stress, $E = 813$ MPa, $\nu = 0.4999$

	asymmetric tensile loading		simple tensile loading	
	$(\Delta u_y, \sigma_y)$	$(\Delta u_x, \sigma_{xy})$	$(\Delta u_y, \sigma_y)$	$(\Delta u_x, \sigma_{xy})$
range of the edge effect	4.6	3.9	4.5	3.4
range of validity of the transmission condition	4.9803	4.9883	4.9803	4.9894
range of the singularity dominated domain	4.999...	4.999...	4.999...	4.999...

Table 10 : Norm verification of the transmission conditions. Plane stress, asymmetrical tensile loading, $E = 813$ MPa, $\nu = 0.4999$

error	interval	$\frac{\|\Delta u_x - a_2 \sigma_{xy}\|_2}{\|\Delta u_x\|_2}$	$\frac{\|\Delta u_y - a_1 \sigma_y\|_2}{\|\Delta u_y\|_2}$
simple	$(-5.00, 5.00)$	$6.563 \cdot 10^{-2}$	$6.876 \cdot 10^{-3}$
loading	$(-4.98, 4.98)$	$2.390 \cdot 10^{-3}$	$5.460 \cdot 10^{-4}$
complex	$(-5.00, 5.00)$	$3.575 \cdot 10^{-2}$	$1.614 \cdot 10^{-2}$
loading	$(-4.98, 4.98)$	$1.778 \cdot 10^{-2}$	$1.153 \cdot 10^{-3}$

3.3 Stiff nonideal interface in dissimilar structure

In this subsection the stiff imperfect interface discussed in the introduction is numerically investigated. For this aim, the same steel-aluminum dissimilar rectangle, but with a thin stiff intermediate layer (elastic constants: $E = 21 \cdot 10^6$ MPa, $\nu = 0.3$), is under consideration. The same simple tensile loading $u_y(x, H/2) = v_y(x) = 1 \cdot d$, $u_x(x, H/2) = v_x(x) = 0$ as in subsection 3.1 has been applied in this case. Corresponding distributions of all components of the displacement and stress along the line A (in the middle line of the sample within the interphase) and along the lines B-D (parallel to the interface) are presented in Fig. 11a and Figs. 12-13, respectively. As it follows from the asymptotic solution (cf. (19)-(21)), the displacements within the interphase should be constant in the direction perpendicular to the interface. This fact is confirmed by FEM-calculations in Figs. 11a-12. On the other hand, according to the obtained numerical results in Fig. 11b, the stress components are also constants, while one can conclude from (36), (38) and (40) that the shear stress should rather change its behavior in direction perpendicular to the interface. There is, nevertheless, a simple explanation of the fact observed in the calculations. Namely, one can notify that $\frac{\partial^2}{\partial x^2} u_x = 0$ at point $x = 0$ due to the symmetry conditions (and it is easy to observe in the numerical calculations presented in Fig. 12). Moreover, from Fig. 13 where stress distributions are shown along different lines parallel to the interface and are lying in and out of the interface, one can conclude that all stress components behave exactly in the way as predicted by asymptotic analysis. In this case, only the validity of the fourth transmission condition from Table 1 is not evident in advance. For this reason, we additionally calculated the jump of the shear stress from different parts of the interface, $[\sigma_{xy}]$, and the second derivative of the displacement u_x normalized by the parameter a_3 due to Table 1. Figure 14 confirms a good agreement between the functions.

The edge effect zone can be easily estimated from Fig. 12b and 13a where one of the displacement components u_y and two stress components σ_x and σ_y practically

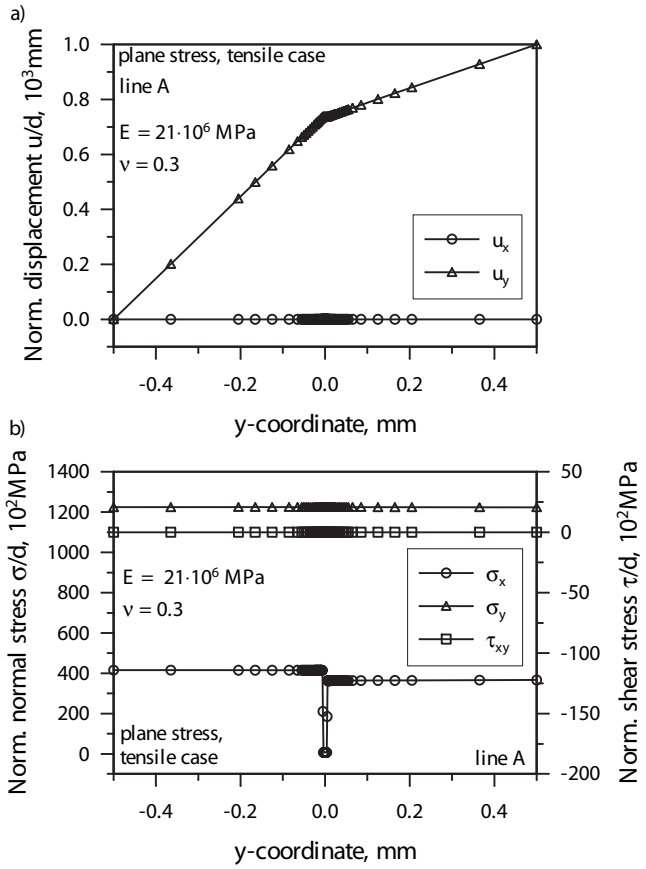

Figure 11 : Displacement and stress distribution along the symmetry axis perpendicular to the interface in the asymmetric sample and the simple tensile loading for the stiff interface

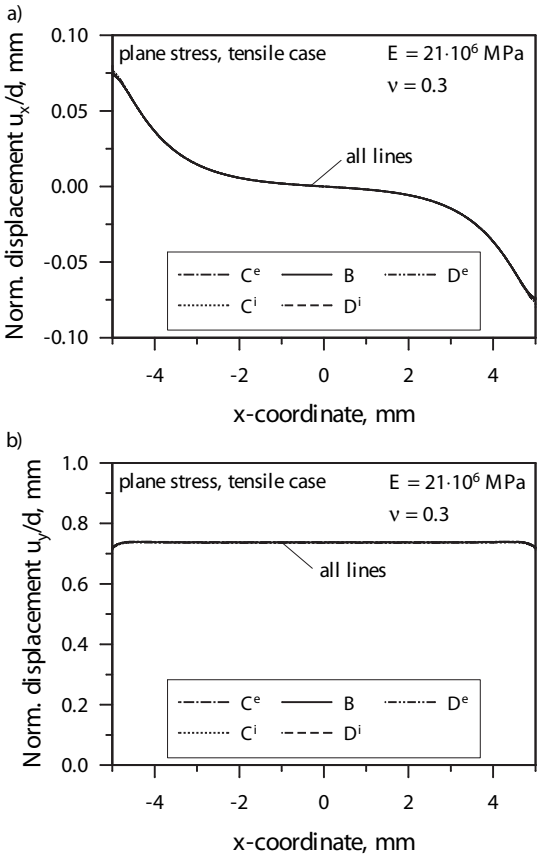

Figure 12 : Displacement distribution along lines B, C and D parallel to the interface in the asymmetric sample and the simple tensile loading for the stiff interface ($d = 1$)

exhibit a constant behavior along the interface. The corresponding distance from the external boundary is even smaller than in the case of the soft interface. To calculate the region where the considered transmission condition is valid, we prepared as earlier a magnification (cf. Fig. 14b) near the right-hand side boundary. Corresponding points on the figure illustrate the respective values. The singularity dominated region is of the same length, while the zone where the transmission condition does not hold true is now two times longer. Moreover, the second derivative of the displacement at the middle line of the interphase ($y = 0$) is bounded near the free boundary. This is an additional proof that the singularity dominated domain is essentially smaller than the thickness of the interface. Otherwise, one should observe a higher growth of the derivative near the free boundary.

Finally, we have also tried to verify the stiff transmission condition in the case of the complex loading which has been introduced in the previous section for the soft interface. However, our FEM-mesh leaded to the same unsatisfactory behavior of the solution, as it has been discussed in the introduction of the first part [Mishuris (2005b)]. This is because bending plays an important role for such loading together with the stiff interface and makes it impossible to use the constructed mesh for the verification of the transmission conditions in this case.

4 Discussions and Conclusions

As it follows from the numerical results by FEM analysis presented here and in paper [Mishuris (2005b)], imperfect transmission conditions for the thin soft and stiff interphases analytically obtained by asymptotic analysis are satisfactory with a very good accuracy even in the case of $\varepsilon = 0.01$. Moreover, in the case of simple symme-

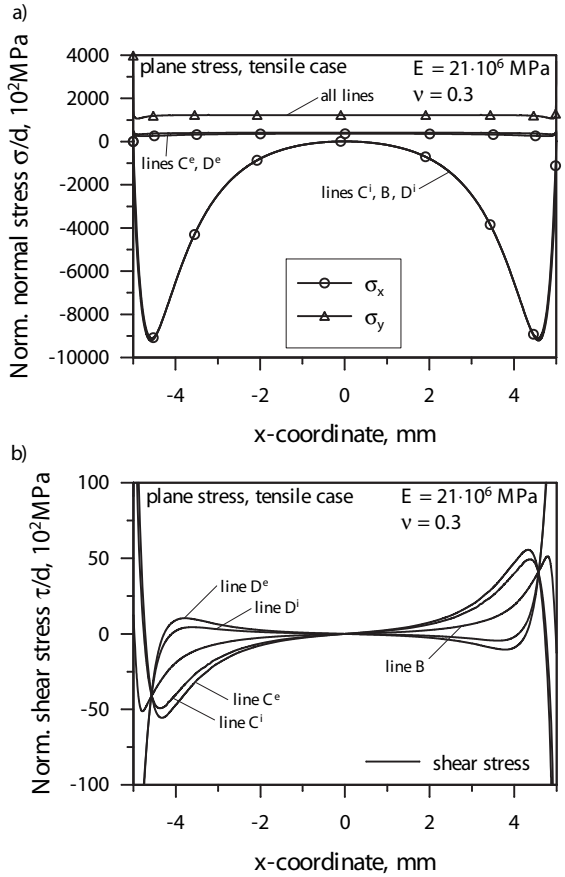

Figure 13 : Normal and shear stress distribution along lines B, C and D parallel to the interface in the asymmetric sample and the simple tensile loading for the stiff interface

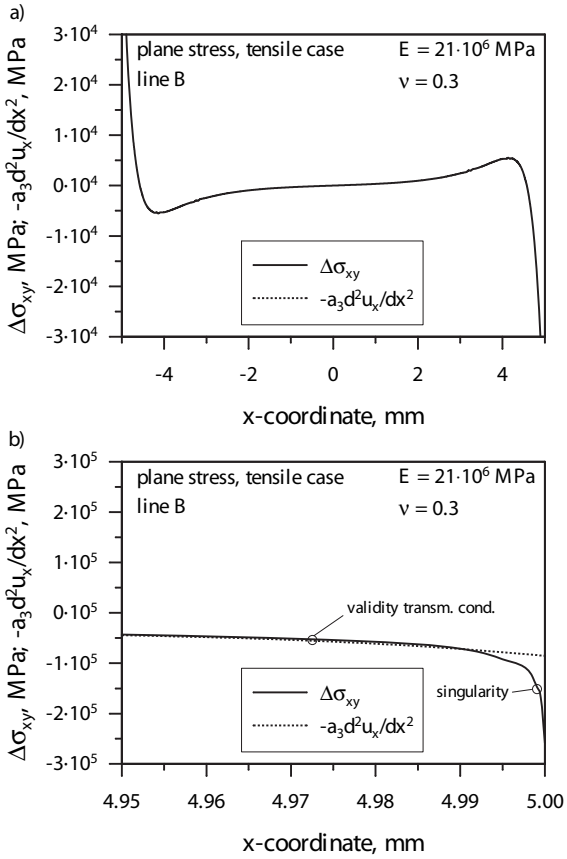

Figure 14 : Verification of the fourth transmission condition for the stiff interface from Table 1 $(d = 1)$

try, the accuracy is essentially better than that predicted by theory. Only in the case of the plane strain problem for the soft weakly compressible interface, the error manifests an essentially different behavior. Let us note that in this case Lamé parameters of the interphase material are not comparable in value and one of the main necessary assumptions to prove the transmission conditions obtained are not valid.

As a result, in the case of the thin intermediate layer between two elastic materials different transmission conditions can be applied depending on relations between the material parameters of the bonded materials and the interphase zone. The question when one can use particular transmission conditions has been answered taking into account relations between the problem parameters. However, it is enough to use, in fact, only two of them - for the stiff and the soft interface. Namely, if the interphase is stiffer than the bonded materials then it makes sense to use the stiff interface transmission conditions, while in the case when the material parameters of the thin layer are smaller than the matched ones then it is necessary to use the transmission conditions for the soft interface. Then in the intermediate case of the comparable in value interface parameters a_j have the same degree $O(\varepsilon)$ with respect to the only small parameter $\varepsilon = h/H$ as the theoretically predicted error.

However, there are still some questions which still remain to be clarified. First, it is necessary to evaluate transmission conditions in the case of the weakly compressible interphase and estimate by the same FEM-analysis the range of their applicability. This phenomenon has been observed in [Ryabenkov (1999)] but no solution has been suggested. On the other hand, it is highly important to estimate an error introduced into final calculations by utilization of any of the proposed imperfect transmission conditions from the initial stage.

Hence, the analysis will be not complete if one does not calculate numerical solutions based on the imperfect transmission conditions and does not compare it with the accurate numerical solutions for the finite thin interface. Moreover, such comparison has been done in the whole domain not only near the imperfect interface. Let us note that the estimates for the zones presented in Table 7 give us the possibility to properly locate special singular and transmission elements of respective sizes in a constructed FEM mesh. These problems will be pointed out in future investigations.

The edge effect appears on a distance comparable with twenty five times the thickness of the interface. In fact, this zone can be considered as a region where Saint-Venant's principle fails. The interesting and important fact is that this zone essentially depends on the type of interface that is not so evident from the first glance. Namely, the size of the edge effect zone monotonically depends on the ratio E/E_{-}. However, the verified transmission conditions fail only on a distance of two interface thickness, while the singularity dominated zone extends on a distance of only $h/100$. Of course, the lengths of the zones are strongly influenced by the chosen criterion. We have applied a 1% accuracy criterion throughout the paper which corresponds to the predicted accuracy of the transmission conditions $O(\varepsilon)$. However, regardless of the criterion choice the region where the transmission conditions are not valid is essentially smaller than the size of the edge zone.

Although FEM analysis is very useful for verification in value in comparison with the formal asymptotic analysis, it has its own restrictions concerning values of the small parameter and strong difficulties connecting with necessity to build a complicated mesh which can be additionally depending on the type of loading, as it occurred in our investigations for bending. Also it is difficult to define an unknown form of corresponding transmission conditions from FEM analysis. However, in the case when one can suppose any specific conditions, they might be numerically verified. In such a way there is a possibility to evaluate imperfect transmission conditions in the case when respective asymptotic analysis is difficult to carry out. Taking this fact into account, we are going to evaluate and verify transmission conditions for thin plastic interphases. First attempt have been done in [Mishuris (2005a)].

Acknowledgement: G. Mishuris is grateful for support provided by the NATO collaborative linkage grant PST.CLG.980398. A. Öchsner is grateful to Portuguese Foundation of Science and Technology for financial support.

References

Akisania, A.R.; Fleck, N. (1997): Interfacial cracking from the free-edge of a long bi-material strip. *Int J Solids Structures*, vol. 34, pp. 1645–1665.

Antipov, Y.A.; Avila-Pozos, O.; Kolaczkowski, S.T.; Movchan, A.B. (2001): Mathematical model of delamination cracks on imperfect interfaces. *Int. J. Solids and Structures*, vol. 38, pp. 6665–6697.

Boichuk, V. (2001): Edge effects in a composite weakly reinforced with fibers of rectangular cross section. *Int Appl Mech*, vol. 37, pp. 682–688.

Kokhanenko, Y.V.; Fesenko, S. (2003): Influence of young's moduli of a laminated composite with a periodic system of cracks on edge effects. *Int Appl Mech*, vol. 39, pp. 99–104.

Li, W.; Siegmund, T. (2004): Numerical study of indentation delamination of strongly bonded films by use of a cohesive zone model. *CMES: Computer Modeling in Engineering & Sciences*, vol. 5, no. 1, pp. 81–90.

Mishuris, G.; Öchsner, A. (2005): Transmission conditions for a soft elasto-plastic interphase between two elastic materials. plane strain state. *Arch Mech*, vol. 57, pp. 157–169.

Mishuris, G.; Öchsner, A.; Kuhn, G. (2005): Fem-analysis of nonclassical transmission conditions between elastic structures. part 1: Soft imperfect interface. *CMC: Computers, Materials & Continua*, vol. 2, pp. 227–238.

Movchan, A.B.; Movhan, N. (1995): *Mathematical Modelling of Solids of with Nonregular Boundaries*. CRC Press, Boca Raton.

Qian, Z.; Akisanya, A. (1998): An experimental investigation of failure initiatian in bonded joints. *Acta Mater*, vol. 46, pp. 4895–4904.

Ryabenkov, N. (1999): On the accuracy of determination of mechanical properties of an adhesive. *Ind Lab*, vol. 65, pp. 124–125.

Yu, H.H.; He, M. H. J. (2001): Edge effects in thin film delamination. *Acta Mater*, vol. 49, pp. 93–107.